PERGAMON

International Journal of Solids and Structures 38 (2001) 241–259

INTERNATIONAL JOURNAL OF SOLIDS and STRUCTURES

www.elsevier.com/locate/ijsolstr

A strip element method for the transient analysis of symmetric laminated plates

Y.Y. Wang *, K.Y. Lam, G.R. Liu

Institute of High Performance Computing, 89C Science Park Drive, # 02-11/12 The Rutherford, Singapore 118261

Received 16 March 1999

Abstract

In this article, an extension of the strip element method has been developed to investigate the transient response of symmetric laminated plates. In this method, the two-dimensional governing equations based on the classical laminated plate theory is reduced to a set of ordinary differential equations using the principle of minimum potential energy. The resulting set of ordinary differential equations are then solved analytically to obtain the dynamic responses in the frequency domain. The Fourier transform technique is then used to obtain the time domain response. An exponential window method is employed to avoid singularities associated with Fourier integration. Transient responses of a rectangular symmetric laminated plate are presented for various loading and boundary conditions. The results obtained using the strip element method were found to compare favorably with exact or analytical solutions available in the literature.

Keywords: Strip element method; Transient analysis; Laminated plate; Dynamic response; Numerical method

1. Introduction

The transient response of laminated composite plates to dynamic loading has received much attention from designers due to increasing applications of composite in high performance aircraft, vehicles and vessels. In the analysis of laminated plates, which are subjected to dynamic loading, the classical laminated plate theory (CLPT) (e.g., Reddy, 1997) is widely used due to its simplicity. More complex plate theories have also been used, such as the first-order shear deformation theory (FSDT) (Whitney, 1969; Whitney and Pagano, 1970; Reissner, 1972), the third-order laminated theory (Reddy, 1984b) and others (Reddy, 1984a,b, 1985).

It is very difficult to obtain the exact solution for the dynamic response of laminated composite plate. Currently, the exact solution can only be available for certain plate theories applied to simply supported rectangular plates (Khdeir and Reddy, 1989). As a result, approximate methods have been proposed for dynamic analysis of the laminated plates.

* Corresponding author.
E-mail address: wangyy@ihpc.nus.edu.sg (Y.Y. Wang).

0020-7683/00/$ - see front matter
PII: S0020-7683(00)00035-4

Currently, most of the works available in the literature are for plates with simply supported boundary conditions. Lu (1996) employed the Rayleigh–Ritz method and the method of superposition of normal modes to calculate the dynamic response of laminated angle-ply plates with clamped boundary conditions which are subjected to explosive loading. However, numerical methods have to be used if the problem involves complex geometries and boundary conditions.

Many numerical methods have been proposed for the dynamic response analysis of plates. Out of these methods, the finite element method (FEM) has become the universally applicable technique for solving boundary and initial value problems. Various types of thin-plate bending elements have been discussed (Zienkiwicz, 1977; Reddy and Miravete, 1995). In the past years, Reismann (1968), Reismann and Lee (1969) and Lee and Reismann (1969) have analyzed simply supported rectangular isotropic plates, which are subjected to suddenly applied uniformly distributed load over a square area on the plate. The transient finite element analysis of isotropic plate was also carried out by Rock and Hinton (1974) for thick and thin plates. Akay (1980) determined the large deflection transient response of isotropic plates using a mixed FEM.

As for composite plates analysis, Reddy (1983) presented finite element results for the transient analysis of layered composite plates based on the FSDT. Mallikarjuna and Kant (1988) presented an isoparametric finite element formulation based on a high-order displacement model for dynamic analysis of multi-layer symmetric composite plate.

Although FEM is an extremely versatile and powerful technique, it has certain disadvantages: large quantities of input data make implementation tedious, and one is often compelled to employ automatic mesh and load generation schemes; many lower order elements will not yield acceptable stress results, necessitating the use of stress averaging or interpolation; and computer core requirement can often be extremely large. Thus, there have been efforts to formulate alternative methods, which lead to the development of the finite strip method (FSM) (Cheung, 1976) and boundary element method (BEM) (Beskos, 1987). The BEM has been successfully used for a great variety of problems, though a major deficiency is that it is difficult to apply for anisotropic and inhomogeneous solids, as there are no simple applicable Green's function available.

Since then, Liu and Achenbach (1994, 1995) proposed the strip element method (SEM) which has been successful in solving plane-strain problems. Subsequently, Wang et al. (1997) developed the SEM for static bending analysis of orthotropic plates. The purpose of this article is to further extend the SEM for transient analysis of symmetric laminated plates. SEM formulations for dynamic analysis of laminated plate were derived, and a SEM program was developed. The program is first used to investigate the dynamic response of the plate in the frequency domain. The Fourier transform technique is then employed to obtain the time domain response, and an exponential window method is introduced to avoid the singularities from Fourier integration. The transient responses of rectangular symmetric laminated plates are presented for various loading and boundary conditions. The results obtained using SEM are compared with exact or analytical solutions. Very good agreements of this comparison were observed.

2. A brief of plate theory for laminates

Consider a thin plate as shown in Fig. 1. The plate consists of K layers of fiber reinforced laminated composite lying in the x–y plane, and the overall thickness is denoted by H. The reference plane $z=0$ is located at the undeformed mid-plane of the plate. The z axis is taken as positive upward from the mid-plane. The kth layer is located between the points $z=z_{k-1}$ and $z=z_k$ in the thickness direction and its principal material coordinate oriented at an angle, α_k, to the laminate coordinate x as shown in Fig. 2.

Let u, v and w denote the displacements in the coordinate directions of x, y and z, respectively. The displacements u and v can be expressed by w according to the following CLPT:

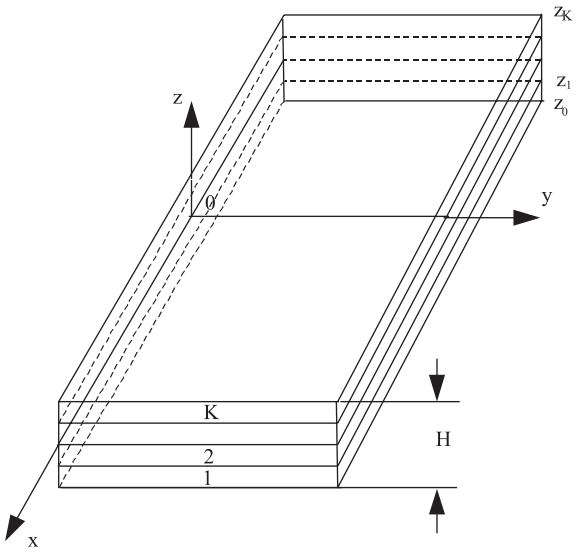

Fig. 1. The coordination system of the composite laminated plate.

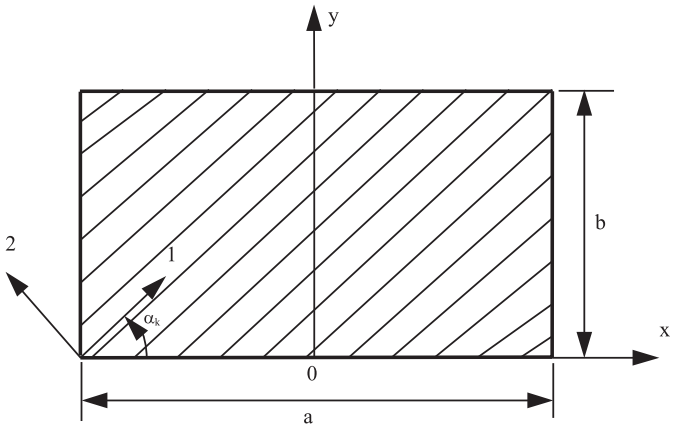

Fig. 2. Geometry and coordination system of the kth layer of a rectangular plate in the x–y plane with fiber orientation of α_k.

$$u = -z\frac{\partial w}{\partial x}, \qquad v = -z\frac{\partial w}{\partial y}. \tag{1}$$

The strain–displacement relations for the plate can be written in the matrix form as

$$\begin{Bmatrix} \varepsilon_x \\ \varepsilon_y \\ \gamma_{xy} \end{Bmatrix} = -z\boldsymbol{L}w, \tag{2}$$

where

$$\boldsymbol{L}^{\mathrm{T}} = \begin{bmatrix} \dfrac{\partial^2}{\partial x^2} & \dfrac{\partial^2}{\partial y^2} & 2\dfrac{\partial^2}{\partial x \partial y} \end{bmatrix} \tag{3}$$

is the differential operator matrix with superscript T denoting transposed matrix.

According to generalized Hooke's law, the stress–strain relation for the kth layer in the laminate coordinates is

$$\begin{Bmatrix} \sigma_x \\ \sigma_y \\ \tau_{xy} \end{Bmatrix}^k = \begin{bmatrix} \bar{Q}_{11} & \bar{Q}_{12} & \bar{Q}_{13} \\ \bar{Q}_{12} & \bar{Q}_{22} & \bar{Q}_{23} \\ \bar{Q}_{13} & \bar{Q}_{23} & \bar{Q}_{33} \end{bmatrix}^k \begin{Bmatrix} \varepsilon_x \\ \varepsilon_y \\ \gamma_{xy} \end{Bmatrix} = \bar{\boldsymbol{Q}}^k \begin{Bmatrix} \varepsilon_x \\ \varepsilon_y \\ \gamma_{xy} \end{Bmatrix}, \tag{4}$$

where $\bar{\boldsymbol{Q}}^k$ is given by

$$\bar{\boldsymbol{Q}}^k = \boldsymbol{T}\boldsymbol{Q}^k\boldsymbol{T}^{\mathrm{T}}, \tag{5}$$

$$\boldsymbol{T} = \begin{bmatrix} l^2 & m^2 & lm \\ m^2 & l^2 & -lm \\ -2lm & 2lm & l^2 - m^2 \end{bmatrix}, \tag{6}$$

$$l = \cos\alpha_k, \qquad m = \sin\alpha_k. \tag{7}$$

In Eq. (5), $\boldsymbol{Q}^k$ is the matrix of material constants for the kth layer in the principal material coordinates with its components are defined as

$$\begin{aligned} &Q_{11} = \frac{E_1}{1 - v_{12}v_{21}}, \qquad Q_{12} = \frac{v_{12}E_2}{1 - v_{12}v_{21}} = \frac{v_{21}E_1}{1 - v_{12}v_{21}}, \qquad Q_{22} = \frac{E_2}{1 - v_{12}v_{21}}, \\ &Q_{66} = G_{12}, \qquad Q_{16} = Q_{26} = 0, \end{aligned} \tag{8}$$

where E_1 and E_2 are Young's moduli in the directions parallel and perpendicular to the fibers, respectively; G_{12} is the shear modulus and v_{12} and v_{21} are Poisson's ratios.

In the present study, only symmetrically stacked laminates are considered. As such, the transverse bending and in-plane stretching are decoupled. The bending moment vector can be written as follows:

$$\begin{Bmatrix} M_x \\ M_y \\ M_{xy} \end{Bmatrix} = -\boldsymbol{D}\boldsymbol{L}w, \tag{9a}$$

$$Q_x = \frac{\partial M_x}{\partial x} + \frac{\partial M_{xy}}{\partial y}, \qquad Q_y = \frac{\partial M_{xy}}{\partial x} + \frac{\partial M_y}{\partial y}, \tag{9b}$$

where the matrix $\boldsymbol{D}$ is the coefficient matrix of the bending stiffness, which is given as

$$\boldsymbol{D} = \begin{bmatrix} D_{11} & D_{12} & D_{16} \\ D_{12} & D_{22} & D_{26} \\ D_{16} & D_{26} & D_{66} \end{bmatrix}, \tag{10}$$

where

$$D_{ij} = \frac{1}{3}\sum_{k=1}^{N} (\bar{Q}_{ij})_k (z_k^3 - z_{k-1}^3). \tag{11}$$

The lateral mid-plane deflection of the thin plate is assumed to satisfy the governing partial differential equation:

$$W = D_{11}\frac{\partial^4 w}{\partial x^4} + 4D_{16}\frac{\partial^4 w}{\partial x^3\,\partial y} + 2(D_{12} + 2D_{66})\frac{\partial^4 w}{\partial x^2\,\partial y^2} + 4D_{26}\frac{\partial^4 w}{\partial x\,\partial y^3} + D_{22}\frac{\partial^4 w}{\partial y^4} + \rho H\frac{\partial^2 w}{\partial t^2} - q = 0, \tag{12}$$

where q is the distributed transverse force on the plate.

3. Formulation of strip element method

To use the SEM in the vibration analysis of a rectangular plate, an infinite length plate is first considered. As shown in Fig. 3, the infinite length plate occupies the region of $-\infty \leqslant x \leqslant \infty$ and $0 \leqslant y \leqslant b$, whereas the problem domain is bounded by $-a/2 \leqslant x \leqslant a/2$, $0 \leqslant y \leqslant b$ and $-H/2 \leqslant z \leqslant H/2$. The boundaries are denoted by S_1, S_2, S_3 and S_4. The infinite plate is divided in the y direction into N strip elements. The displacement field in an element is assumed to be of the form:

$$w = \boldsymbol{N}(y)\boldsymbol{V}^{\mathrm{e}}(x,t), \tag{13}$$

where matrix $\boldsymbol{N}(y)$ and vector $\boldsymbol{V}^{\mathrm{e}}(x)$ are given by

$$\boldsymbol{N}(y) = [\, n_1(y) \quad n_2(y) \quad n_3(y) \quad n_4(y) \quad n_5(y) \quad n_6(y) \,], \tag{14}$$

$$\begin{aligned}\boldsymbol{V}^{\mathrm{e}}(x,t) &= [\, w_1(x,t) \quad \theta_1(x,t) \quad w_2(x,t) \quad \theta_2(x,t) \quad w_3(x,t) \quad \theta_3(x,t) \,]^{\mathrm{T}} \\ &= [\, v_1(x,t) \quad v_2(x,t) \quad v_3(x,t) \quad v_4(x,t) \quad v_5(x,t) \quad v_6(x,t) \,]^{\mathrm{T}}\end{aligned} \tag{15}$$

and w_i $(i = 1,2,3)$ are the lateral deflections on the node lines. θ_i $(i = 1,2,3)$ are the rotation angles on the node lines as given by $\theta_i = \partial w/\partial y|_{y=y_i}$. The elements in matrix $\boldsymbol{N}(y)$ are obtained using Hermite interpolation functions (Wang et al., 1997):

$$\begin{aligned}
n_1(y) &= 1 - 23\frac{y^2}{b_{\mathrm{e}}^2} + 66\frac{y^3}{b_{\mathrm{e}}^3} - 68\frac{y^4}{b_{\mathrm{e}}^4} + 24\frac{y^5}{b_{\mathrm{e}}^5}, \\
n_2(y) &= y\left(1 - 6\frac{y}{b_{\mathrm{e}}} + 13\frac{y^2}{b_{\mathrm{e}}^2} - 12\frac{y^3}{b_{\mathrm{e}}^3} + 4\frac{y^4}{b_{\mathrm{e}}^4}\right), \\
n_3(y) &= 16\frac{y^2}{b_{\mathrm{e}}^2} - 32\frac{y^3}{b_{\mathrm{e}}^3} + 16\frac{y^4}{b_{\mathrm{e}}^4}, \\
n_4(y) &= y\left(-8\frac{y}{b_{\mathrm{e}}} + 32\frac{y^2}{b_{\mathrm{e}}^2} - 40\frac{y^3}{b_{\mathrm{e}}^3} + 16\frac{y^4}{b_{\mathrm{e}}^4}\right), \\
n_5(y) &= 7\frac{y^2}{b_{\mathrm{e}}^2} - 34\frac{y^3}{b_{\mathrm{e}}^3} + 52\frac{y^4}{b_{\mathrm{e}}^4} - 24\frac{y^5}{b_{\mathrm{e}}^5}, \\
n_6(y) &= y\left(-\frac{y}{b_{\mathrm{e}}} + 5\frac{y^2}{b_{\mathrm{e}}^2} - 8\frac{y^3}{b_{\mathrm{e}}^3} + 4\frac{y^4}{b_{\mathrm{e}}^4}\right),
\end{aligned} \tag{16}$$

where b_{e} is the width of the strip element.

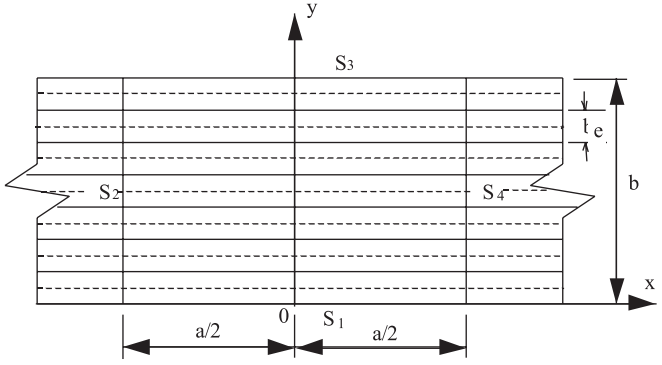

Fig. 3. The infinite plate is divided to strip elements in y direction, whereas the region bounded by S_1, S_2, S_3 and S_4 is the problem domain.

Generally, the term, W, in Eq. (12) is not zero when the displacement field is expressed as in Eq. (13). By applying the principle of minimum potential energy to the strip element in the infinite plate, we obtain the following equation:

$$\int_0^{b_e} W\,\delta w\,\mathrm{d}y + \boldsymbol{R}_y\,\delta \boldsymbol{V}^e(x,t) = \boldsymbol{T}\,\delta \boldsymbol{V}^e(x,t), \tag{17}$$

where

$$\boldsymbol{R}_y = \left[-\left(\frac{\partial M_{yx}}{\partial x} + Q_y\right)\Big|_{y=0} \quad M_y\big|_{y=0} \quad 0 \quad 0 \quad \left(\frac{\partial M_{yx}}{\partial x} + Q_y\right)\Big|_{y=b_e} \quad -M_y\big|_{y=b_e} \right] \tag{18}$$

and $\boldsymbol{T}$ is the external traction vector acting on the boundary lines of the element. Using Eqs. (9) and (12), (13), (17) and (18), we can obtain a set of approximate ordinary differential equations for an element (Wang et al., 1997):

$$\boldsymbol{B}_1^e \frac{\partial^4 \boldsymbol{V}^e}{\partial x^4} + \boldsymbol{B}_2^e \frac{\partial^3 \boldsymbol{V}^e}{\partial x^3} + \boldsymbol{B}_3^e \frac{\partial^2 \boldsymbol{V}^e}{\partial x^2} + \boldsymbol{B}_4^e \frac{\partial \boldsymbol{V}^e}{\partial x} + \boldsymbol{B}_5^e \boldsymbol{V}^e + \boldsymbol{B}_6^e \frac{\partial^2 \boldsymbol{V}^e}{\partial t^2} - \boldsymbol{F}^e = \boldsymbol{T}^e. \tag{19}$$

In the above expression, the matrices $\boldsymbol{B}_1^e$, $\boldsymbol{B}_3^e$, $\boldsymbol{B}_5^e$ and $\boldsymbol{B}_6^e$ are symmetric, whereas $\boldsymbol{B}_2^e$ and $\boldsymbol{B}_4^e$ are anti-symmetric. The coefficient matrices $\boldsymbol{B}_i^e$ ($i = 1$–6) and force vector $\boldsymbol{F}^e$ due to the distributed load q are shown in Appendix A. By assembling all the strip elements of the domain, a system of approximate ordinary differential equations for the whole domain can be obtained:

$$\boldsymbol{B}_1 \frac{\partial^4 \boldsymbol{V}}{\partial x^4} + \boldsymbol{B}_2 \frac{\partial^3 \boldsymbol{V}}{\partial x^3} + \boldsymbol{B}_3 \frac{\partial^2 \boldsymbol{V}}{\partial x^2} + \boldsymbol{B}_4 \frac{\partial \boldsymbol{V}}{\partial x} + \boldsymbol{B}_5 \boldsymbol{V} + \boldsymbol{B}_6 \frac{\partial^2 \boldsymbol{V}}{\partial t^2} = \boldsymbol{P} \tag{20}$$

in which $\boldsymbol{P} = \boldsymbol{F} + \boldsymbol{T}$, and $\boldsymbol{T}$ expresses the vector of concentrated force on the node line. The matrices $\boldsymbol{B}_i$ ($i = 1$–6) and $\boldsymbol{F}$ can be obtained by assembling the corresponding matrices of adjacent elements as in the FEM. If the plate is divided into N strip elements, then $\boldsymbol{B}_i$ ($i = 1$–6) will be $M \times M$ ($M = 4N + 2$) matrices.

4. Solution in the frequency domain

Eq. (20) is a set of fourth-order differential equations, where $\boldsymbol{V}$ and $\boldsymbol{P}$ are functions of x and t. To solve this equation, the Fourier transformation with respect to the time t is introduced:

$$\tilde{\boldsymbol{V}}(x,\omega) = \int_{-\infty}^{\infty} \boldsymbol{V}(x,t) \mathrm{e}^{-\mathrm{i}\omega t}\,\mathrm{d}t, \tag{21}$$

$$\tilde{\boldsymbol{P}}(x,\omega) = \int_{-\infty}^{\infty} \boldsymbol{P}(x,t) \mathrm{e}^{-\mathrm{i}\omega t}\,\mathrm{d}t, \tag{22}$$

where ω is the angular frequency and "$\sim$" stands for a variable in the frequency domain. Application of the Fourier transform to Eq. (20) leads to the following ordinary differential equation:

$$\boldsymbol{B}_1 \frac{\mathrm{d}^4 \tilde{\boldsymbol{V}}}{\mathrm{d}x^4} + \boldsymbol{B}_2 \frac{\mathrm{d}^3 \tilde{\boldsymbol{V}}}{\mathrm{d}x^3} + \boldsymbol{B}_3 \frac{\mathrm{d}^2 \tilde{\boldsymbol{V}}}{\mathrm{d}x^2} + \boldsymbol{B}_4 \frac{\mathrm{d} \tilde{\boldsymbol{V}}}{\mathrm{d}x} + \boldsymbol{B}_5 \tilde{\boldsymbol{V}} - \omega^2 \boldsymbol{B}_6 \tilde{\boldsymbol{V}} = \tilde{\boldsymbol{P}}. \tag{23}$$

This equation can be solved analytically. Its general solution has two parts, which are the complementary solution which satisfies the associated homogeneous equation of Eq. (23), and the particular solution which satisfies Eq. (23).

4.1. Complementary solution

The complementary solution can be obtained by solving the associated homogeneous equation of Eq. (23) ($\tilde{\boldsymbol{P}} = 0$). Assuming

$$\tilde{\boldsymbol{V}} = \boldsymbol{d}_0 \exp(\mathrm{i}kx) \tag{24}$$

and substituting it into the homogeneous equation of Eq. (23). Thus, we have the following equation:

$$(k^4\boldsymbol{B}_1 - \mathrm{i}k^3\boldsymbol{B}_2 - k^2\boldsymbol{B}_3 + \mathrm{i}k\boldsymbol{B}_4 + \boldsymbol{B}_5 - \omega^2\boldsymbol{B}_6)\boldsymbol{d}_0 = 0. \tag{25}$$

This equation can be converted to a standard eigenvalue equation with respect to k:

$$\begin{bmatrix} 0 & \boldsymbol{I} & 0 & 0 \\ 0 & 0 & \boldsymbol{I} & 0 \\ 0 & 0 & 0 & \boldsymbol{I} \\ -\boldsymbol{B}_5 + \omega^2\boldsymbol{B}_6 & -\mathrm{i}\boldsymbol{B}_4 & \boldsymbol{B}_3 & \mathrm{i}\boldsymbol{B}_2 \end{bmatrix} \begin{Bmatrix} \boldsymbol{d}_0 \\ k\boldsymbol{d}_0 \\ k^2\boldsymbol{d}_0 \\ k^3\boldsymbol{d}_0 \end{Bmatrix} = k \begin{bmatrix} \boldsymbol{I} & 0 & 0 & 0 \\ 0 & \boldsymbol{I} & 0 & 0 \\ 0 & 0 & \boldsymbol{I} & 0 \\ 0 & 0 & 0 & \boldsymbol{B}_1 \end{bmatrix} \begin{Bmatrix} \boldsymbol{d}_0 \\ k\boldsymbol{d}_0 \\ k^2\boldsymbol{d}_0 \\ k^3\boldsymbol{d}_0 \end{Bmatrix}. \tag{26}$$

Eq. (26) can be solved to obtain $4M$ eigenvalues k_j $(j = 1, 2, \ldots, 4M)$ and eigenvectors, which are the functions of ω. The first quarter of the jth eigenvectors corresponds to vector $\boldsymbol{d}_0$, and is denoted by vector $\boldsymbol{\Phi}_j(\omega)$, where

$$\boldsymbol{\Phi}_j^{\mathrm{T}}(\omega) = \{\, \phi_{j1} \quad \phi_{j2} \quad \cdots \quad \phi_{jM} \,\}. \tag{27}$$

The complementary solution for the displacement can be written by superposition of these eigenvectors as shown below:

$$\tilde{\boldsymbol{V}}^{\mathrm{c}}(x,\omega) = \sum_{j=1}^{4M} C_j(\omega)\boldsymbol{\Phi}_j(\omega)\exp(\mathrm{i}k_j x) = \boldsymbol{G}(x,\omega)\boldsymbol{C}(\omega), \tag{28}$$

where superscript c indicates the complementary solution and

$$\boldsymbol{G}(x,\omega) = \begin{bmatrix} \phi_{11}\exp(\mathrm{i}k_1x) & \phi_{21}\exp(\mathrm{i}k_2x) & \cdots & \phi_{L1}\exp(\mathrm{i}k_Lx) \\ \phi_{12}\exp(\mathrm{i}k_1x) & \phi_{22}\exp(\mathrm{i}k_2x) & \cdots & \phi_{L2}\exp(\mathrm{i}k_Lx) \\ \vdots & \vdots & \ddots & \vdots \\ \phi_{1M}\exp(\mathrm{i}k_1x) & \phi_{2M}\exp(\mathrm{i}k_2x) & \cdots & \phi_{LM}\exp(\mathrm{i}k_Lx) \end{bmatrix} \tag{29}$$

with $L = 4M$. In Eq. (28), $\boldsymbol{C}$ is a constant vector, which will be determined by using the boundary conditions on S_2 and S_4 after the particular solution is obtained.

4.2. Particular solution

In order to obtain the particular solution of Eq. (23), the Fourier transformation with respect to coordinate x is introduced as follows:

$$\bar{\tilde{\boldsymbol{V}}}^{\mathrm{p}}(k,\omega) = \int_{-\infty}^{\infty} \tilde{\boldsymbol{V}}^{\mathrm{p}}(x,\omega)\mathrm{e}^{-\mathrm{i}kx}\,\mathrm{d}x, \tag{30}$$

$$\bar{\tilde{\boldsymbol{P}}}^{\mathrm{p}}(k,\omega) = \int_{-\infty}^{\infty} \tilde{\boldsymbol{P}}^{\mathrm{p}}(x,\omega)\mathrm{e}^{-\mathrm{i}kx}\,\mathrm{d}x, \tag{31}$$

where superscript p indicates the particular solution and "–"stands for a variable in the transform domain. Application of the Fourier transform to Eq. (23) leads to the following equation in the transform domain:

$$\bar{\tilde{\boldsymbol{P}}} = [k^4\boldsymbol{B}_1 - \mathrm{i}k^3\boldsymbol{B}_2 - k^2\boldsymbol{B}_3 + \mathrm{i}k\boldsymbol{B}_4 + \boldsymbol{B}_5 - \omega^2\boldsymbol{B}_6]\bar{\tilde{\boldsymbol{V}}}^{\mathrm{p}}. \tag{32}$$

This equation can be rewritten as

$$\boldsymbol{p} = [\boldsymbol{A} - k\boldsymbol{B}]\boldsymbol{d}, \tag{33}$$

where

$$\boldsymbol{p} = \left\{ 0 \quad 0 \quad 0 \quad -\bar{\tilde{\boldsymbol{P}}}^{\mathrm{T}} \right\}^{\mathrm{T}}, \qquad \boldsymbol{d} = \left\{ \bar{\tilde{\boldsymbol{V}}}^{\mathrm{pT}} \quad k\bar{\tilde{\boldsymbol{V}}}^{\mathrm{pT}} \quad k^2\bar{\tilde{\boldsymbol{V}}}^{\mathrm{pT}} \quad k^3\bar{\tilde{\boldsymbol{V}}}^{\mathrm{pT}} \right\}^{\mathrm{T}}, \tag{34}$$

$$\boldsymbol{A} = \begin{bmatrix} 0 & \boldsymbol{I} & 0 & 0 \\ 0 & 0 & \boldsymbol{I} & 0 \\ 0 & 0 & 0 & \boldsymbol{I} \\ -\boldsymbol{B}_5 + \omega^2\boldsymbol{B}_6 & -\mathrm{i}\boldsymbol{B}_4 & \boldsymbol{B}_3 & \mathrm{i}\boldsymbol{B}_2 \end{bmatrix}, \qquad \boldsymbol{B} = \begin{bmatrix} \boldsymbol{I} & 0 & 0 & 0 \\ 0 & \boldsymbol{I} & 0 & 0 \\ 0 & 0 & \boldsymbol{I} & 0 \\ 0 & 0 & 0 & \boldsymbol{B}_1 \end{bmatrix}. \tag{35}$$

Applying the modal analysis technique (Liu and Achenbach, 1995), we arrive at

$$\boldsymbol{d} = \sum_{m=1}^{4M} \frac{\phi_m^{\mathrm{L}}\boldsymbol{p}\phi_m^{\mathrm{R}}}{(k_m - k)B_m}, \tag{36}$$

where

$$B_m = \phi_m^{\mathrm{L}}\boldsymbol{B}\phi_m^{\mathrm{R}} \tag{37}$$

and the eigenvalues k_m, left eigenvectors ϕ_m^{L} and right eigenvectors ϕ_m^{R} corresponding to the homogeneous equation (33) can obtained by solving the following equations:

$$\phi_m^{\mathrm{L}}[\boldsymbol{A} - k_m\boldsymbol{B}] = 0, \qquad [\boldsymbol{A} - k_m\boldsymbol{B}]\phi_m^{\mathrm{R}} = 0. \tag{38}$$

The ϕ_m^{R} and ϕ_m^{L} can be partitioned in the form of

$$\phi_m^{\mathrm{R}} = \begin{Bmatrix} \phi_{m1}^{\mathrm{R}} \\ \phi_{m2}^{\mathrm{R}} \\ \phi_{m3}^{\mathrm{R}} \\ \phi_{m4}^{\mathrm{R}} \end{Bmatrix}, \qquad \phi_m^{\mathrm{L}} = \left\{ \phi_{m1}^{\mathrm{L}} \quad \phi_{m2}^{\mathrm{L}} \quad \phi_{m3}^{\mathrm{L}} \quad \phi_{m4}^{\mathrm{L}} \right\}, \tag{39}$$

where ϕ_{mi}^{R} $(i = 1, 2, 3, 4)$ and ϕ_{mj}^{L} $(j = 1, 2, 3, 4)$ have the same dimension. From Eqs. (34), (36) and (39), we obtain

$$\bar{\tilde{\boldsymbol{V}}}^{\mathrm{p}}(k, \omega) = -\sum_{m=1}^{4M} \frac{\phi_{m4}^{\mathbf{L}}\bar{\tilde{\boldsymbol{P}}}\phi_{m1}^{\mathbf{R}}}{(k_m - k)B_m}. \tag{40}$$

Once the external load is specified, the vector of the load Fourier transformation $\bar{\tilde{\boldsymbol{P}}}$ can then be obtained. By applying the inverse Fourier transformation to Eq. (40), the particular solution of Eq. (23) can be obtained as

$$\tilde{\boldsymbol{V}}^{\mathrm{p}}(x, \omega) = \frac{1}{2\pi}\int_{-\infty}^{\infty} \bar{\tilde{\boldsymbol{V}}}^{\mathrm{p}}(k, \omega)\mathrm{e}^{ikx}\mathrm{d}k = \frac{1}{2\pi}\int_{-\infty}^{\infty} \sum_{m=1}^{4M} \frac{\phi_{m4}^{\mathrm{L}}\bar{\tilde{\boldsymbol{P}}}\phi_{m1}^{\mathrm{R}}}{(k - k_m)B_m}\mathrm{e}^{\mathrm{i}kx}\,\mathrm{d}k. \tag{41}$$

The general solution of Eq. (23) is the sum of the complementary solution given by Eq. (28) and the particular solution given by Eq. (41):

$$\tilde{\boldsymbol{V}}(x, \omega) = \tilde{\boldsymbol{V}}^{\mathrm{c}}(x, \omega) + \tilde{\boldsymbol{V}}^{\mathrm{p}}(x, \omega) = \boldsymbol{G}(x, \omega)\boldsymbol{C}(\omega) + \tilde{\boldsymbol{V}}^{\mathrm{p}}(x, \omega). \tag{42}$$

4.3. Determination of constant vector $\boldsymbol{C}$ using boundary conditions

Eq. (42) gives the fundamental solution for the infinite plate, in which the constant vector $\boldsymbol{C}$ with $4M$ elements is unknown. To obtain a special solution for the problem domain, the boundary conditions on S_2 and S_4 have to be used to determine the constant vector $\boldsymbol{C}$. There are $2N+1$ node lines and two boundary conditions on each node line can be obtained from the CLPT. The boundary conditions in CLPT are summarized as follows:

$$w = 0, \qquad \frac{\partial w}{\partial x} = 0 \quad \text{(for the clamped edges)}, \tag{43}$$

$$w = 0 \qquad \frac{\partial^2 w}{\partial x^2} = 0 \quad \text{(for simply supported boundary)}. \tag{44}$$

As for free boundary conditions, it follows that

$$M_x = 0, \qquad \frac{\partial M_{xy}}{\partial y} + Q_x = 0. \tag{45}$$

Therefore, there are only $2M$ boundary conditions on S_2 and S_4, which is insufficient to determine the $4M$ constants. Additional $2M$ boundary conditions are therefore needed. Wang et al. (1997) developed the boundary conditions in SEM for orthotropic plates, where the additional boundary conditions to be introduced are

$$\theta = 0, \qquad \frac{\partial \theta}{\partial x} = 0 \quad \text{(for clamped boundary)}, \tag{46}$$

$$\theta = 0, \qquad \frac{\partial^2 \theta}{\partial x^2} = 0 \quad \text{(for simply supported boundary)}, \tag{47}$$

$$\frac{\partial M_x}{\partial y} = 0, \qquad \frac{\partial}{\partial y}\left(\frac{\partial M_{xy}}{\partial y} + Q_x\right) = 0 \quad \text{(for free boundary)}. \tag{48}$$

It can be shown that these boundary conditions can also be applied in this work; thus, the boundary conditions in SEM are summarized as follows:

Clamped supported boundary

$$\tilde{\boldsymbol{V}} = 0, \qquad \frac{\mathrm{d}\tilde{\boldsymbol{V}}}{\mathrm{d}x} = 0. \tag{49}$$

Simply supported boundary

$$\tilde{\boldsymbol{V}} = 0, \qquad \frac{\mathrm{d}^2\tilde{\boldsymbol{V}}}{\mathrm{d}x^2} = 0. \tag{50}$$

Free boundary

$$\tilde{\boldsymbol{M}}_x = 0, \quad \frac{\partial \tilde{\boldsymbol{M}}_{xy}}{\partial y} + \tilde{\boldsymbol{Q}}_x = 0, \quad \frac{\partial \tilde{\boldsymbol{M}}_x}{\partial y} = 0, \quad \frac{\partial}{\partial y}\left(\frac{\partial \tilde{\boldsymbol{M}}_{xy}}{\partial y} + \tilde{\boldsymbol{Q}}_x\right) = 0, \tag{51}$$

where the vectors express the corresponding values on the node lines in the frequency domain. Hence, the constant vector $\boldsymbol{C}$ can be determined using the above boundary conditions, which gives the exact number of boundary conditions. Thus, the responses in the frequency domain can successfully be obtained.

5. Solution in the time domain

The inverse Fourier transformation to Eq. (42) gives the solution in the time domain:

$$\boldsymbol{V}(x,t) = \frac{1}{2\pi}\int_{-\infty}^{\infty} \tilde{\boldsymbol{V}}(x,\omega)\mathrm{e}^{\mathrm{i}\omega t}\mathrm{d}\omega. \tag{52}$$

The integration of Eq. (52) usually has to be carried out numerically. However, for the undamped plates as considered in this article, difficulties with the integration result from singularities of $\tilde{\boldsymbol{V}}(x,\omega)$ at $\omega = 0$ and at the cut-off frequencies ($k = 0$), as discussed by Vasudevan and Mal (1985). To overcome these difficulties, the exponential window method (EWM) is used. Liu and Achenbach (1994) calculated the response of wave scattering in an infinite plate using the EWM. The basic idea of the EWM is to introduce a complex frequency, $\omega - \mathrm{i}\eta$, by adding to it a small imaginary part, $\mathrm{i}\eta$, where ω is real and η is positive and does not depend on ω. Hence, the Fourier transform pair given by Eqs. (21) and (52) can equivalently be written as

$$\tilde{\boldsymbol{V}}(x,\omega - \mathrm{i}\eta) = \int_{-\infty}^{\infty} \mathrm{e}^{-\eta t}\boldsymbol{V}(x,t)\mathrm{e}^{-\mathrm{i}\omega t}\,\mathrm{d}t, \tag{53}$$

$$\boldsymbol{V}(x,t) = \frac{\mathrm{e}^{\eta t}}{2\pi}\int_{-\infty}^{\infty} \tilde{\boldsymbol{V}}(x,\omega - \mathrm{i}\eta)\mathrm{e}^{\mathrm{i}\omega t}\,\mathrm{d}\omega, \tag{54}$$

and the Fourier transform of external force in Eq. (22) is

$$\tilde{\boldsymbol{P}}(x,\omega - \mathrm{i}\eta) = \int_{-\infty}^{\infty} \mathrm{e}^{-\eta t}\boldsymbol{P}(x,t)\mathrm{e}^{-\mathrm{i}\omega t}\,\mathrm{d}t. \tag{55}$$

It is to be noted that the ω in Eqs. (23)–(42) should be replaced by $\omega - \mathrm{i}\eta$.

Generally, the external force is loaded on the plate only for a certain time duration in the transient analysis; thus, Eq. (55) takes the form

$$\tilde{\boldsymbol{P}}(x,\omega - \mathrm{i}\eta) = \int_{0}^{t_d} \mathrm{e}^{-\eta t}\boldsymbol{P}(x,t)e^{-\mathrm{i}\omega t}\,\mathrm{d}t, \tag{56}$$

where t_d is the duration of the external force. Eq. (54) is used to obtain the displacement response in the time domain, which avoids the singularity of $\tilde{\boldsymbol{V}}(x,\omega)$.

6. Numerical examples

The transient analyses of anisotropic laminated composite plates are carried out by using a SEM program written in FORTRAN 77. In the present study, zero initial conditions are assumed.

Example 1. Considering a three-layer cross-ply (0°/90°/0°) square laminated plate, where all layers are assumed to be of the same thicknesses and material properties. The material properties are given as

$$E_1 = 172.369\ \text{GPa}, \quad E_2 = 6.895\ \text{GPa}, \quad G_{12} = 3.448\ \text{GPa}, \quad \nu_{12} = 0.25, \quad \rho = 1603.03\ \text{kg/m}^3.$$

The total thickness of the plate is taken to be $H = 3.81$ cm, and the length of the plate is $a = b = 20H$.

The load is sinusoidally distributed on the whole surface of the plate and varies with time according to one of the expressions given below:

$$q(x,y,t) = q_0 \sin\pi\left(\frac{1}{2} - \frac{x}{a}\right)\sin\frac{\pi y}{b}F(t), \tag{57}$$

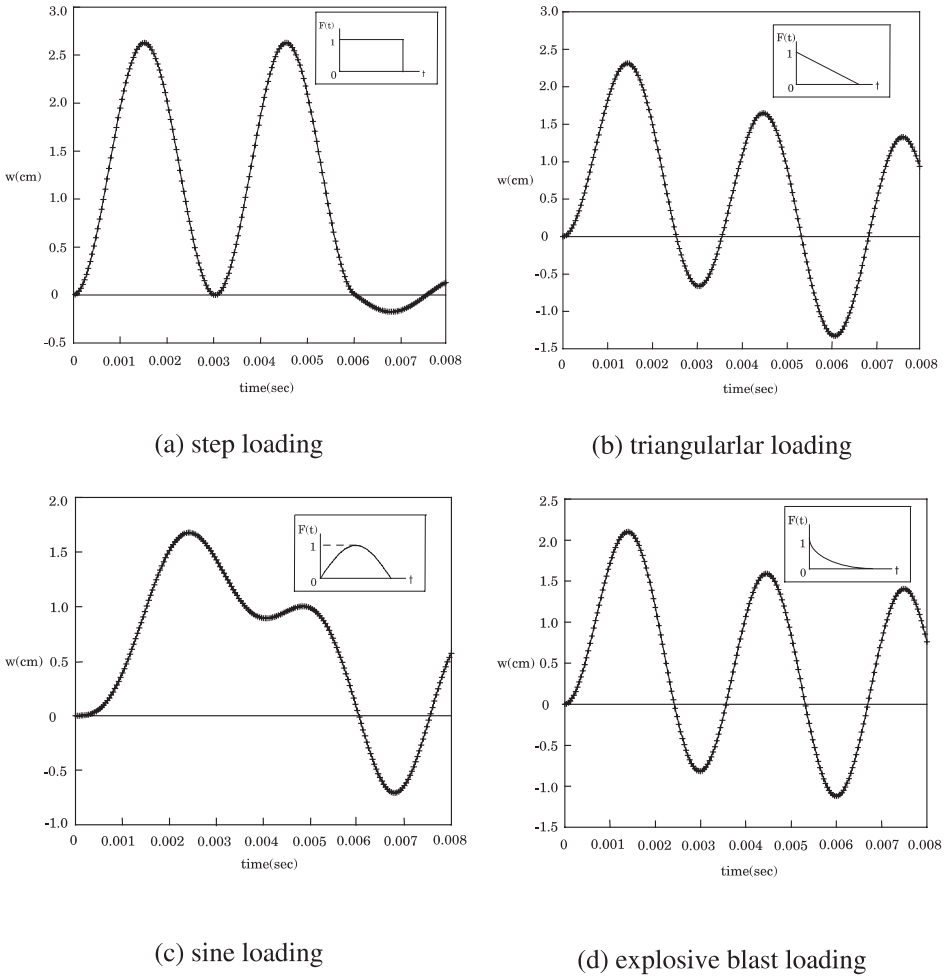

Fig. 4. Time history of the center deflection for simple supported [0°/90°/0°] square laminated plate under various loading. A comparison of the SEM solution (the real line) and exact solution (the cross).

$$F(t)=\begin{cases}\left\{\begin{matrix}\sin(\pi t/t_1) & 0\leqslant t_1\\ 0 & t>t_1\end{matrix}\right\} & \text{sine loading,}\\ \left\{\begin{matrix}1 & 0\leqslant t\leqslant t_1\\ 0 & t>t_1\end{matrix}\right\} & \text{step loading,}\\ \left\{\begin{matrix}(1-t/t_1) & 0\leqslant t\leqslant t_1\\ 0 & t>t_1\end{matrix}\right\} & \text{triangular loading,}\\ \mathrm{e}^{-\gamma t} & \text{explosive blast loading,}\end{cases} \tag{58}$$

in which $t_1 = 0.006$ s and $\gamma = 330\ \mathrm{s}^{-1}$. The intensity of the transverse load is taken to be $q_0 = 3.448$ MPa.

The integration in Eq. (41) for a line load acting at $x = x_0$ can be easily obtained using Cauchy's theorem (Wang et al., 1997), and the particular solution is given as

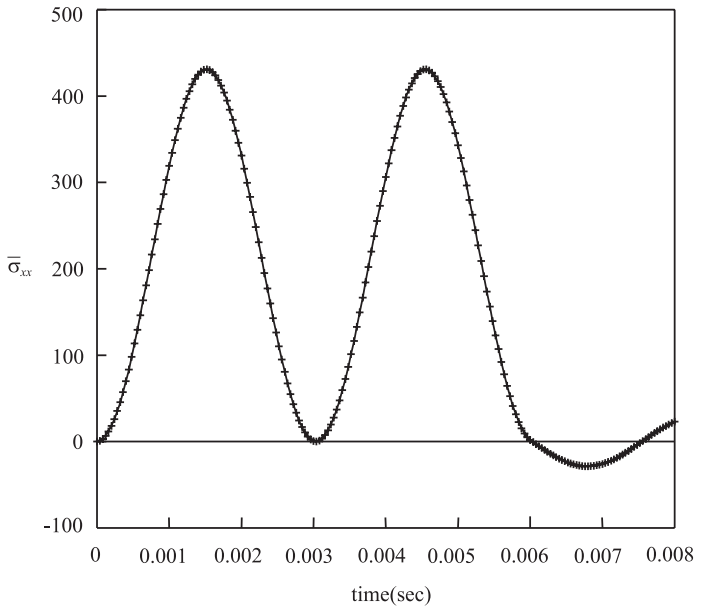

Fig. 5. The time history of the dimensionless normal stress $\bar{\sigma}_{xx}$ versus time for simple supported [0°/90°/0°] square laminated plate under step loading. Comparison of the SEM solution (the real line) and exact solution (the cross).

$$\tilde{\boldsymbol{V}}^{\mathrm{p}}(x,\omega)=\begin{cases}\displaystyle\sum_{m=1}^{2M}\mathrm{i}\frac{\phi_{m4}^{\mathrm{L}+}\tilde{\boldsymbol{P}}\phi_{m1}^{\mathrm{R}+}}{\boldsymbol{B}_m^{+}}\mathrm{e}^{\mathrm{i}k_m^{+}(x-x_0),} & x\geqslant x_0\\ \displaystyle\sum_{m=1}^{2M}-\mathrm{i}\frac{\phi_{m4}^{\mathrm{L}-}\tilde{\boldsymbol{P}}\phi_{m1}^{\mathrm{R}-}}{\boldsymbol{B}_m^{-}}\mathrm{e}^{\mathrm{i}k_m^{-}(x-x_0),} & x<x_0\end{cases}\tag{59}$$

where "+" denotes variables corresponding to the positive real eigenvalues or complex eigenvalues with positive imaginary part, whereas "−" denotes variables evaluated for the other cases of the eigenvalues.

In the case of a distributed load in the x direction

$$p(x,y,t)=f(x)p(y,t),\tag{60}$$

the particular solution can be obtained from the following integration:

$$\tilde{\boldsymbol{V}}^{\mathrm{p}}=\int_{-a/2}^{x}f(x)\sum_{m=1}^{2M}\mathrm{i}\frac{\phi_{m4}^{\mathrm{L}+}\tilde{\boldsymbol{P}}\phi_{m1}^{\mathrm{R}+}}{\boldsymbol{B}_m^{+}}\mathrm{e}^{\mathrm{i}k_m^{+}(x-x_0)}\,\mathrm{d}x+\int_{x}^{a/2}f(x)\sum_{m=1}^{2M}-\mathrm{i}\frac{\phi_{m4}^{\mathrm{L}-}\tilde{\boldsymbol{P}}\phi_{m1}^{\mathrm{R}-}}{\boldsymbol{B}_m^{-}}\mathrm{e}^{\mathrm{i}k_m^{-}(x-x_0)}\,\mathrm{d}x.\tag{61}$$

Thus, the particular solution for the sinusoidally distributed load expressed by Eq. (57) can be carried out using Eq. (61), which is given as:

$$\begin{aligned}\tilde{\boldsymbol{V}}^{\mathrm{p}}=&\sum_{m=1}^{2M}\mathrm{i}\frac{\phi_{m4}^{\mathrm{L}^-}\tilde{\boldsymbol{P}}\phi_{m1}^{\mathrm{R}^-}}{B_m^{-}}\frac{\frac{\pi}{a}\sin\frac{\pi x}{a}-\mathrm{i}k_m^{-}\cos\frac{\pi x}{a}-\frac{\pi}{a}\mathrm{e}^{\mathrm{i}k_m^{-}(x-a/2)}}{-(k_m^{-})^2+\left(\frac{\pi}{a}\right)^2}\\&+\sum_{m=1}^{2M}\mathrm{i}\frac{\phi_{m4}^{\mathrm{L}^+}\tilde{\boldsymbol{P}}\phi_{m1}^{\mathrm{R}^+}}{B_m^{+}}\frac{\frac{\pi}{a}\sin\frac{\pi x}{a}-\mathrm{i}k_m^{+}\cos\frac{\pi x}{a}+\frac{\pi}{a}\mathrm{e}^{\mathrm{i}k_m^{+}(x+a/2)}}{-(k_m^{+})^2+(\frac{\pi}{a})^2}.\end{aligned}\tag{62}$$

Fig. 4 shows the time history of the transverse deflection at the center of the plate for various loads. The comparisons of the SEM results with exact solutions (Khdeir and Reddy, 1989) are shown. From Fig. 4, it is observed that the SEM solutions are in very good agreement with the exact solutions.

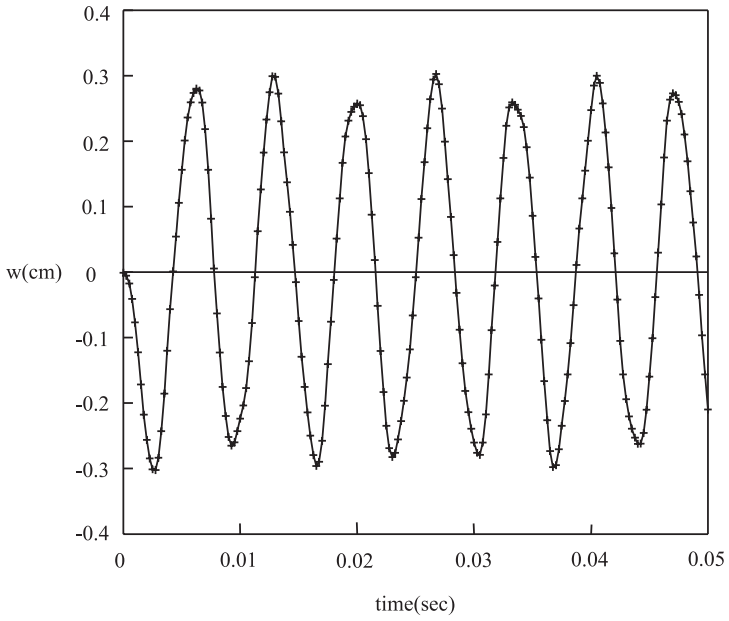

Fig. 6. The time history of the deflection on the center of the [30°/−30°/−30°/30°] square laminated plate, which is fully clamped and subjects to conventional blast. Comparison of SEM solution (the real line) and Rayleigh–Ritz solution (the cross).

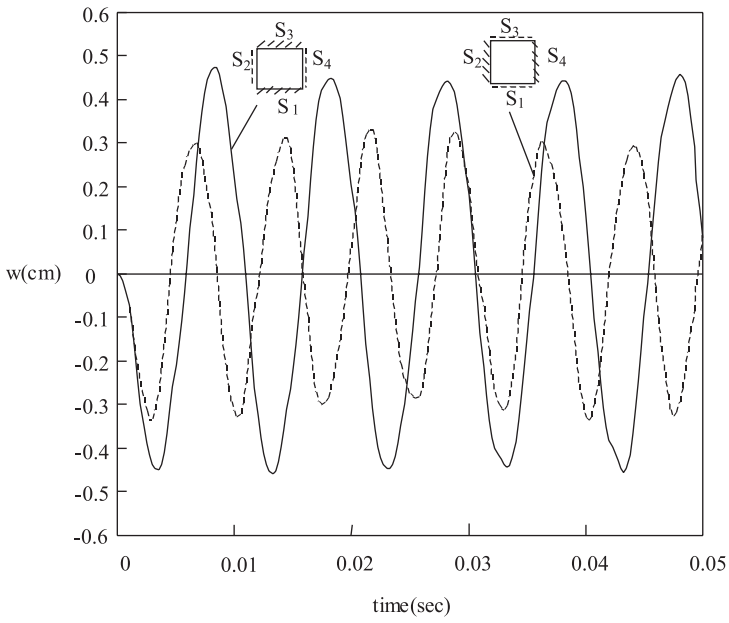

Fig. 7. The time history of the center deflection of the [30°/−30°/−30°/30°] square laminated plate which subjects to conventional blast. The plate is clamped at two opposite edges and simply supported at the other two edges.

The stress responses in the time domain can be obtained from the displacement distribution using a similar method as for the deflection response. The normal stress response in time domain for sine loading and the comparison of SEM solutions with exact solutions are given in Fig. 5, in which the dimensionless normal stress is defined as

$$\bar{\sigma}_{xx} = \sigma_{xx}(a/2, b/2, H/2)/q_0. \tag{63}$$

Again, a very good agreement is achieved. It can be seen that the stress response curve is very similar to the displacement response curve. This conclusion is similar for other load cases.

Example 2. A four-layer angle-ply square laminated plate with symmetrically stacking sequences (30°/−30°/−30°/30°) is considered. All layers are assumed to have the same thicknesses and material properties given by

$$E_1 = 131.69 \text{ GPa}, \quad E_2 = 8.55 \text{ GPa}, \quad G_{12} = 6.67 \text{ GPa}, \quad v_{12} = 0.3, \quad \rho = 1610 \text{ kg/m}^{-3}.$$

The dimensions of the plate are

$$a_1 = 1.27 \text{ m}, \quad b_1 = 1.27 \text{ m}, \quad H = 0.0254 \text{ m}.$$

The plate is subjected to a conventional blast while the pressure can be considered uniformly distributed over the plate, which can be expressed as

$$q(x, y, t) = q_0\left(1 - \frac{t}{t_p}\right)e^{-\alpha t/t_p}, \tag{64}$$

where the parameters in Eq. (64) are taken as

$$\alpha = 1.98, \quad t_p = 4 \text{ ms}, \quad q_0 = 68.95 \text{ kPa}.$$

These data are taken from Lu (1996).

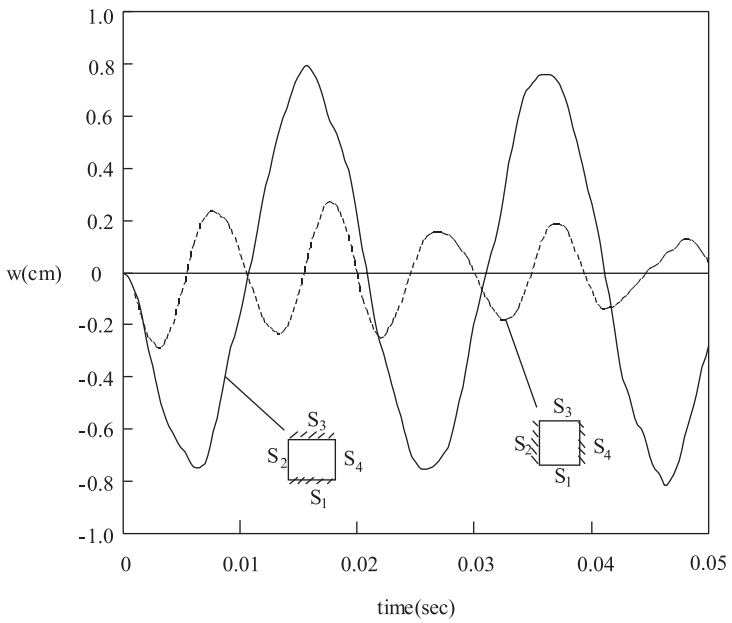

Fig. 8. As in Fig. 7, but the plate is clamped at two opposite edges and free at the other two edges.

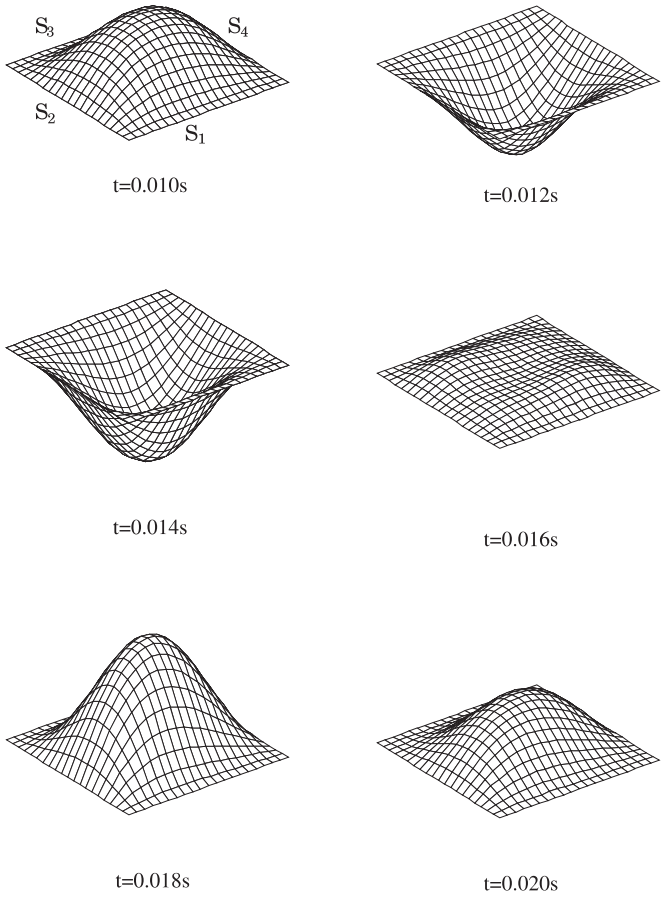

Fig. 9. The deflection of the [30°/−30°/−30°/30°] square laminated plate which subjects to conventional blast. The plate is clamped on edges S_1 and S_3 and simply supported on edges S_2 and S_4.

For the uniformly distributed external load along the x axis, the particular solution in Eq. (41) is given as

$$\tilde{\boldsymbol{V}}^{\mathrm{p}} = \sum_{m=1}^{2M} \frac{\phi_{m4}^{\mathrm{L}+} \tilde{\boldsymbol{P}} \phi_{m1}^{\mathrm{R}+}}{\boldsymbol{B}_m^+} \frac{\mathrm{e}^{\mathrm{i}k_m^+(x+a/2)} - 1}{k_m^+} + \sum_{m=1}^{2M} \frac{\phi_{m4}^{\mathrm{L}-} \tilde{\boldsymbol{P}} \phi_{m1}^{\mathrm{R}-}}{\boldsymbol{B}_m^-} \frac{\mathrm{e}^{\mathrm{i}k_m^-(x-a/2)} - 1}{k_m^-}. \tag{65}$$

The results for the fully clamped plate are shown in Fig. 6. The comparison with Lu's results using Rayleigh–Ritz method shows a good agreement.

The effects of the boundary conditions of composite laminated plates have been shown in Figs. 7 and 8. Fig. 7 shows the deflection versus time of the square composite laminated plate for two boundary condition cases: (1) S_1 and S_3 clamped, S_2 and S_4 simply supported; (2) S_1 and S_3 simply supported, S_2 and S_4 clamped.

It is known that the deflection and frequency of a square isotropic plate are the same for the above two boundary condition cases. However, this is not true in the case of composite laminated plates, in which both the deflection and frequency are different for the two types of boundary conditions. This fact can also been found from Fig. 8, in which two boundary condition cases for the square composite laminated plate are: (1) S_1 and S_3 clamped, S_2 and S_4 free; (2) S_1 and S_3 free, S_2 and S_4 clamped.

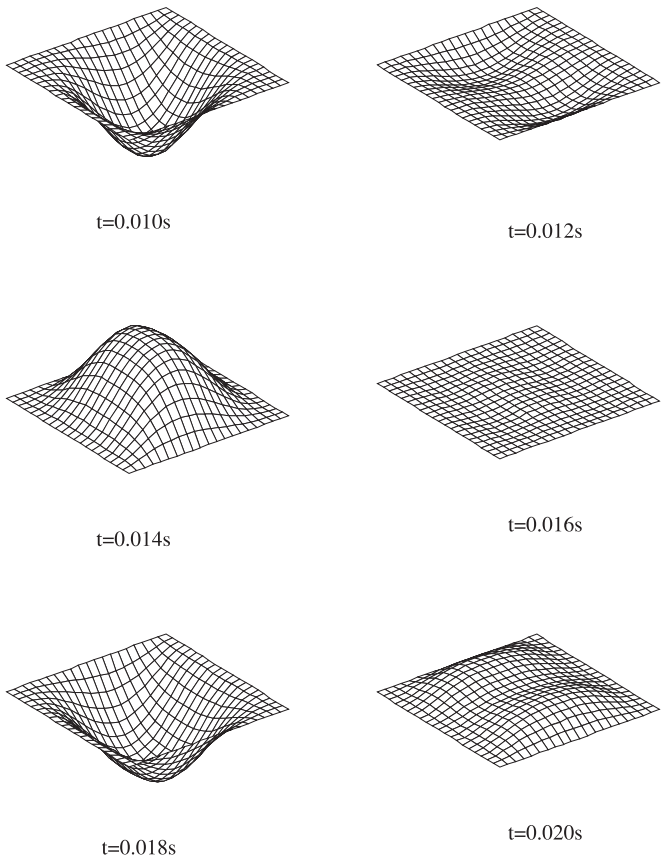

Fig. 10. As in Fig. 9, but the plate is simply supported on S_1 and S_3 and clamped on S_2 and S_4.

The deformation of the plate at different times is shown in Figs. 9 and 10, in which the plate was clamped on two opposite edges and simply supported on the other two edges. In these figures, the transverse deformations have been increased in scale. It is found that the deformation distribution is different for those two types of boundary conditions also. From the above discussion, it is concluded that the composite laminated plates must be designed carefully according to the boundary conditions of the practical applications.

7. Discussion and conclusions

The SEM for the dynamic analysis of laminated composite plates has been presented based on the CLPT. This method has many advantages:

1. It requires a small memory during computation.
2. It requires fewer elements to achieve the required accuracy. In this article, only four elements are used.
3. The SEM achieves a high accuracy as both deflection and rotation angle are continuous along the node lines.

4. Generally the integration in Eq. (41) for a distributed load of a given function can be carried out analytically. This also improves the accuracy of the SEM solution.

When the SEM is applied to transient analysis of laminated composite plates, the Fourier transform technique is used to investigate dynamic response in the frequency domain, and the time domain response is obtained using the inverse Fourier transformation. An exponential window method is introduced to avoid singularities in the Fourier integration. Numerical solutions obtained for laminated composite plates with various loading and boundary conditions indicate that SEM is a very accurate numerical method.

Appendix A

Matrices in Eq. (19):

$$\boldsymbol{B}_1^{\mathrm{e}} = D_{11}\begin{bmatrix} \frac{523b_{\mathrm{e}}}{3465} & \frac{19b_{\mathrm{e}}^2}{2310} & \frac{4b_{\mathrm{e}}}{63} & \frac{-8b_{\mathrm{e}}^2}{693} & \frac{131b_{\mathrm{e}}}{6930} & \frac{-29b_{\mathrm{e}}^2}{13860} \\ & \frac{2b_{\mathrm{e}}^3}{3465} & \frac{2b_{\mathrm{e}}^2}{315} & \frac{-b_{\mathrm{e}}^3}{1155} & \frac{29b_{\mathrm{e}}^2}{13860} & \frac{-b_{\mathrm{e}}^3}{4620} \\ & & \frac{12b_{\mathrm{e}}}{315} & 0 & \frac{4b_{\mathrm{e}}}{63} & \frac{-2b_{\mathrm{e}}^2}{315} \\ & & & \frac{32b_{\mathrm{e}}^3}{3465} & \frac{8b_{\mathrm{e}}^2}{693} & \frac{-b_{\mathrm{e}}^3}{1155} \\ & \text{sym} & & & \frac{523b_{\mathrm{e}}}{3465} & \frac{-19b_{\mathrm{e}}^2}{2310} \\ & & & & & \frac{2b_{\mathrm{e}}^3}{3465} \end{bmatrix},$$

$$\boldsymbol{B}_2^{\mathrm{e}} = 4D_{16}\begin{bmatrix} 0 & \frac{23b_{\mathrm{e}}}{630} & \frac{8}{21} & \frac{-32b_{\mathrm{e}}}{315} & \frac{5}{42} & \frac{-b_{\mathrm{e}}}{90} \\ & 0 & \frac{8b_{\mathrm{e}}}{315} & \frac{-2b_{\mathrm{e}}^2}{315} & \frac{b_{\mathrm{e}}}{90} & \frac{-b_{\mathrm{e}}^2}{1260} \\ & & 0 & \frac{64b_{\mathrm{e}}}{315} & \frac{8}{21} & \frac{-8b_{\mathrm{e}}}{315} \\ & \text{asy} & & 0 & \frac{32b_{\mathrm{e}}}{315} & \frac{-2b_{\mathrm{e}}^2}{315} \\ & & & & 0 & \frac{23b_{\mathrm{e}}}{630} \\ & & & & & 0 \end{bmatrix},$$

$$\boldsymbol{B}_3^{\mathrm{e}} = 2D_{12}\begin{bmatrix} \frac{-278}{105b_{\mathrm{e}}} & \frac{-118}{210} & \frac{256}{105b_{\mathrm{e}}} & \frac{-8}{21} & \frac{22}{105b_{\mathrm{e}}} & \frac{1}{70} \\ & \frac{-2b_{\mathrm{e}}}{45} & \frac{-8}{105} & \frac{4b_{\mathrm{e}}}{315} & \frac{-1}{70} & \frac{b_{\mathrm{e}}}{126} \\ & & \frac{-512}{105b_{\mathrm{e}}} & 0 & \frac{256}{105b_{\mathrm{e}}} & \frac{-8}{105} \\ & & & \frac{-128b_{\mathrm{e}}}{315} & \frac{8}{21} & \frac{4b_{\mathrm{e}}}{315} \\ & \text{sym} & & & \frac{-278}{105b_{\mathrm{e}}} & \frac{118}{210} \\ & & & & & \frac{-2b_{\mathrm{e}}}{45} \end{bmatrix}$$

$$+ 4D_{66}\begin{bmatrix} \frac{-278}{105b_{\mathrm{e}}} & \frac{-13}{210} & \frac{256}{105b_{\mathrm{e}}} & \frac{-8}{21} & \frac{22}{105b_{\mathrm{e}}} & \frac{1}{70} \\ & \frac{-2b_{\mathrm{e}}}{45} & \frac{-8}{105} & \frac{4b_{\mathrm{e}}}{315} & \frac{-1}{70} & \frac{b_{\mathrm{e}}}{126} \\ & & \frac{-512}{105b_{\mathrm{e}}} & 0 & \frac{256}{105b_{\mathrm{e}}} & \frac{-8}{105} \\ & & & \frac{-128b_{\mathrm{e}}}{315} & \frac{8}{21} & \frac{4b_{\mathrm{e}}}{315} \\ & \text{sym} & & & \frac{-278}{105b_{\mathrm{e}}} & \frac{13}{210} \\ & & & & & \frac{-2b_{\mathrm{e}}}{45} \end{bmatrix},$$

$$\boldsymbol{B}_4^{\mathrm{e}} = 4D_{26}\begin{bmatrix} 0 & \frac{-79}{35b_{\mathrm{e}}} & \frac{32}{7b_{\mathrm{e}}^2} & \frac{128}{35b_{\mathrm{e}}} & \frac{-32}{7b_{\mathrm{e}}^2} & \frac{31}{35b_{\mathrm{e}}} \\ & 0 & \frac{-48}{35b_{\mathrm{e}}} & \frac{32}{35} & \frac{-31}{35b_{\mathrm{e}}} & \frac{11}{70} \\ & & 0 & \frac{-256}{35b_{\mathrm{e}}} & \frac{32}{7b_{\mathrm{e}}^2} & \frac{48}{35b_{\mathrm{e}}} \\ & & & 0 & \frac{-128}{35b_{\mathrm{e}}} & \frac{32}{35} \\ & \text{asy} & & & 0 & \frac{-79}{35b_{\mathrm{e}}} \\ & & & & & 0 \end{bmatrix},$$

$$\boldsymbol{B}_5^{\mathrm{e}} = D_{22}\begin{bmatrix} \frac{5092}{35b_{\mathrm{e}}^3} & \frac{1138}{35b_{\mathrm{e}}^2} & \frac{-512}{5b_{\mathrm{e}}^3} & \frac{384}{7b_{\mathrm{e}}^2} & \frac{-1058}{35b_{\mathrm{e}}^3} & \frac{242}{35b_{\mathrm{e}}^2} \\ & \frac{332}{35b_{\mathrm{e}}} & \frac{-128}{5b_{\mathrm{e}}^2} & \frac{64}{7b_{\mathrm{e}}} & \frac{242}{35b_{\mathrm{e}}^2} & \frac{38}{35b_{\mathrm{e}}} \\ & & \frac{1024}{5b_{\mathrm{e}}^3} & 0 & \frac{-512}{5b_{\mathrm{e}}^3} & \frac{128}{5b_{\mathrm{e}}^2} \\ & & & \frac{256}{7b_{\mathrm{e}}} & \frac{-384}{7b_{\mathrm{e}}^2} & \frac{64}{7b_{\mathrm{e}}} \\ & \text{sym} & & & \frac{5092}{35b_{\mathrm{e}}^3} & \frac{-1138}{35b_{\mathrm{e}}^2} \\ & & & & & \frac{332}{35b_{\mathrm{e}}} \end{bmatrix},$$

$$\boldsymbol{B}_6^{\mathrm{e}} = \rho H\begin{bmatrix} \frac{523b_{\mathrm{e}}}{3465} & \frac{19b_{\mathrm{e}}^2}{2310} & \frac{4b_{\mathrm{e}}}{63} & \frac{-8b_{\mathrm{e}}^2}{693} & \frac{131b_{\mathrm{e}}}{6930} & \frac{-29b_{\mathrm{e}}^2}{13860} \\ & \frac{2b_{\mathrm{e}}^3}{3465} & \frac{2b_{\mathrm{e}}^2}{315} & \frac{-b_{\mathrm{e}}^3}{1155} & \frac{29b_{\mathrm{e}}^2}{13860} & \frac{-b_{\mathrm{e}}^3}{4620} \\ & & \frac{128b_{\mathrm{e}}}{315} & 0 & \frac{4b_{\mathrm{e}}}{63} & \frac{-2b_{\mathrm{e}}^2}{315} \\ & & & \frac{32b_{\mathrm{e}}^3}{3465} & \frac{8b_{\mathrm{e}}^2}{693} & \frac{-b_{\mathrm{e}}^3}{1155} \\ & \text{sym} & & & \frac{523b_{\mathrm{e}}}{3465} & \frac{-19b_{\mathrm{e}}^2}{2310} \\ & & & & & \frac{2b_{\mathrm{e}}^3}{3465} \end{bmatrix}.$$

The elements of vector $\boldsymbol{F}^{\mathrm{e}}$ in Eq. (19):

$$F_i^{\mathrm{e}} = \int_0^{b_{\mathrm{e}}} q(y)n_i(y)\,\mathrm{d}y.$$

References

Akay, H.U., 1980. Dynamic larger deflection analysis of plates using mixed finite elements. Computers and Structures 11, 1–11.

Beskos, D.E., 1987. Boundary Element Method in Mechanics. North-Holland, Amsterdam.

Cheung, Y.K., 1976. The Finite Strip Method in Structural Analysis, Pergamon Press, Oxford.

Khdeir, A.A., Reddy, J.N., 1989. Exact solution for the transient response of symmetric cross-ply laminates using a higher-order plate theory. Composite Science and Technology 34, 205–224.

Lee, Y., Reismann, H., 1969. Dynamics of rectangular plates. International Journal of Engineering Science 7, 93–113.

Liu, G.R., Achenbach, J.D., 1994. A strip element method for stress analysis of anisotropic linearly elastic solid. ASME Journal of Applied Mechanics 61, 270–277.

Liu, G.R., Achenbach, J.D., 1995. Strip element method to analyze wave scattering by cracks in anisotropic laminated plates. ASME Journal of Applied Mechanics 62, 607–613.

Lu, C., 1996. Computational modeling of composite structures and low-velocity impact. Ph.D. Thesis, National University of Singapore.

Mallikarjuna, Kant, T., 1988. Dynamics of laminated composite plates with a higher order theory and finite element discretization. Journal of Sound and Vibration 126, 463–475.

Reddy, J.N., 1983. Dynamic (transient) analysis of layered anisotropic composite-material plates. International Journal for Numerical Methods in Engineering 19, 237–255.

Reddy, J.N., 1984a. A refined nonlinear theory of plates with transverse shear deformation. International Journal of Solids and Structures 20, 881–896.

Reddy, J.N., 1984b. A simple higher-order theory for laminated composite plates. ASME Journal of Applied Mechanics 51, 745–752.

Reddy, J.N., 1985. A review of the literature on finite-element modeling of laminated composite plates. The Shock and Vibration Digest 17, 3–8.

Reddy, J.N., Miravete, A., 1995. Practical Analysis of Laminated Structures. CRC Press, Boca Raton, FL.

Reddy, J.N., 1997. Mechanics of Laminated Composite Plate: Theory and Analysis. CRC Press, Boca Raton, FL.

Reismann, H., 1968. Forced motion of elastic plates. Journal of Applied Mechanics 35, 510–515.

Reismann, H., Lee, Y., 1969. Forced motion of rectangular plates. In: Frederick, D. (Ed.), Development in Theoretical and Applied Mechanics, vol. 4. Pergamon Press, New York, pp. 3–18.

Reissner, E., 1972. A consistent treatment of transverse shear deformations in laminated anisotropic plates. AIAA Journal 10, 716–718.

Rock, T., Hinton, E., 1974. Free vibration and transient response of thick and thin plates using the finite element method. In: Earthquake Engineering and Structural Dynamics, vol. 3. pp. 51–63.

Vasudevan, N., Mal, A.K., 1985. Response of an elastic plate to localized transient source. ASME Journal of Applied Mechanics 52, 356–362.

Wang, Y.Y., Lam, K.Y., Liu, G.R., Reddy, J.N., Tani, J., 1997. A strip element method for bending analysis of orthotropic plates. JSME International Journal A 40, 398–406.

Whitney, J.M., 1969. The effect of transverse shear deformation in the bending of laminated plates. Journal of Composite Materials 3, 534–547.

Whitney, J.M., Pagano, N.J., 1970. Shear deformation in heterogeneous anisotropic plates. ASME Journal of Applied Mechanics 37, 1031–1036.

Zienkiwicz, O.C., 1977. The Finite Element Method. McGraw-Hill, New York.